OPTIMIZATION METHOD TO ESTIMATE BREAST TUMOUR PARAMETERS

Shazzat Hossain and Farah A. Mohammadi
Department of Electrical and Computer Engineering
Ryerson University, 350 Victoria Street, M5B2K3, Toronto, Ontario, Canada
fmohamma@ee.ryerson.ca

ABSTRACT

This paper presents a methodology to predict location, size and hyperactivity level of a breast tumor using temperature profile over the skin surface of the breast that may be captured by infrared thermography or numeric simulation. The estimation methodology includes an evolutionary technique based on artificial neural network (ANN), an optimization scheme based on pattern search algorithm (PSA) with linear constraints and a heat flow analysis on anatomic-accurate (realistic) breast model using finite element method (FEM). Laboratory generated datasets obtained from the FEM are applied to the ANN to associate underlying tumor with surface temperature of the model. The ANN training/testing results are in good agreement with those obtained from numeric method (FEM), thus validates the network performance. The PSA is applied for generation of solution vector sets (tumor parameters) within a given space and the solution sets are employed to produce simulated datasets using the trained ANN. The best solution set is determined by minimizing a cost function involving comparing the target temperature profiles (clinical data) to those obtained by simulation.

KEY WORDS

Bio-heat transfer, breast model, tumor parameter estimation, inverse problem, artificial neural network (ANN), pattern search optimization.

1. Introduction

Breast cancer, the most common cancer among adult women, is a global concern for its gradual increasing incidence rate. Not to mention those who are still undiagnosed, the survival rate of medicated patients is only 22%, if treatment is given at stage-IV [1]. Out of nine Canadian women, anticipated by the Canadian Breast Cancer Foundation (CBCF) in 2013 that, one will develop breast cancer during lifetime while the mortality rate would be one in every twenty nine of them; even though the mortality rate has declined by 42 percent since the peak in 1986 for earlier exposure through routinized mammogram, modernized diagnostic (screening) systems, and improved treatments. Obviously, earlier detections of cancers have been proven particularly fruitful, mainly, for increasing likelihood of more treatment options, consequently, higher survival rates; hence become an important feature in cancer control efforts. Infrared (IR) thermogram, a promising non-invasive functional imager of tumors at earlier stage, has been widely used since the mid-nineties though its preliminary purpose was limited only to screening. Thermogram assesses surface temperature which is controlled by the rate of blood circulation underneath the skin, local metabolism, and heat exchange between the skin and environment [2-4]. Changes any of these parameters can influence the local temperature and heat losses at the skin surface reflecting the physiological state of the human body. Tumor's architecture and angiogenesis process can lead to an abnormal situation; in particular, some features such as the inflammation, metabolic rate, interstitial hypertension, etc. are force the tumor to behave differently than healthy tissue in relation to heat production and dissipation. Surface temperature of a developed malignancy breast may be found a fraction to several degrees higher than the surrounding area [5]. Therefore, the abnormality in skin surface temperature can be explored and utilized for estimating the location, size and thermal parameters of the tumor region as well as to follow up the tumor treatment procedure.

Application of thermography in the breast cancer exposure was proposed in [6] for the first time, while the author observed that the temperatures emanated from the tumor toward the skin was considerably higher (about 2-3 degrees) than the healthy tissues. The regional temperature inconsistency resulting of the embedded tumor was associated with convection effect which was linked with augmented blood perfusion and metabolism all over the tumor [7]. Combining with the direct associations, several inverse bio-thermal models, however, were suggested for estimating thermo-physical parameters of a tumor from surface temperature profiles. Neglecting the thermal effect due to the blood perfusion, a cylindrical adipose thermal model was developed and in-vitro thermal data was captured while heating-up the adipose with a spherical metal ball (tumor model) using a resistive heater and then the thermal dataset was applied to a genetic algorithm (GA) based evolutionary process to predict the depth and heat source power [8]. The authors discovered that the surface temperature exhibits very poor sensitivity to the location of the heat source, especially for a low power heat source, i.e. the depth estimation of benign was inaccurate. Incorporating the perfusion effect, a subsequent evolutionary study (using

DOI: 10.2316/J.2014.216.818-0005

ANN) [9] estimated the location, size and heat generation rate of hot nodule (tumor) embedded in breast utilizing an idealized 2-D breast model proposed in [10] where the train vectors for the ANN were obtained from the numeric simulation of heat transfer equations on the model and then the tumor parameters were predicated with Genetic Algorithm (GA) optimization. However, the estimation methodology was general and require real breast model prior to clinical application.

The objective of this study is proposing a methodology for estimating the depth, size and metabolic rate of an embedded tumor in the lobule region of breast. In order to come up with the goal, a realistic thermal model mimicking the breast geometry and heterogeneity has been developed and heat flow problems are addressed using finite element method (FEM) to generate training vectors for ANN [11]. The train network is then simulated by the predicated parameters which are obtained by optimizing the cost function using the pattern search algorithm (PSM).

Outline of the paper is the following: the mathematical model proposed to simulate the thermal features of breast is discussed in section 2, in addition, discretization of breast into five different domains (chest wall, muscle, fat, lobule and skin) to produce heterogeneous model mimicking the true anatomical structure, furthermore, linking the domains with assorted boundary conditions are presented in this section. Development of the finite element model and generation of ideal dataset for training a neural network are presented in section 3. In section 4, the solution of inverse problems in noiseless and noisy ($\leq\pm10\%$) conditions have been presented and the estimated bio-thermal and physical parameters of breast tumors obtained from pattern search method in ideal and realistic cases are exposed. To summarize, some comments and conclusions are pointed out in section 5.

2. Mathematical Model

Pennes', in 1948, developed a bio-heat transfer model including the conductive heat transfer toward surface, the volumetric metabolic heat generation of the tissue and the heat loss due to blood perfusion which is proportional to the product of the difference between the arterial blood temperature and the local tissue temperature, and the volumetric perfusion rate [12]. The model governs by a time varying second order differential equation, though computing temperature distribution requiring for thermal treatment the following steady-state Pennes' bio-heat equation is required.

$$\lambda_i \nabla^2 T_i(r) + k_i[T_b - T_i(r)] + Q_{mi} = 0 \qquad (1)$$

where the subscript i recognizes the subdomain ($i = 1, 2, 3, \ldots\ldots$), λ_i is the thermal conductivity, $k_i = \omega_{bi} c_{bi}$ is the perfusion coefficient (ω_b and c_b is the volumetric perfusion rate and specific heat of blood, respectively), Q_{mi} is the metabolic heat rate and T_b is the artier blood temperature. Hence, according the model, tissue temperature T is a function of conductive heat flow rate, blood flow rate, specific heat of blood and metabolic rate and these parameters are unlike in different tissues layer. Therefore accurately identifying the layers (domains) and their sizes, and shapes play an important role in finding thermal feature of an organ.

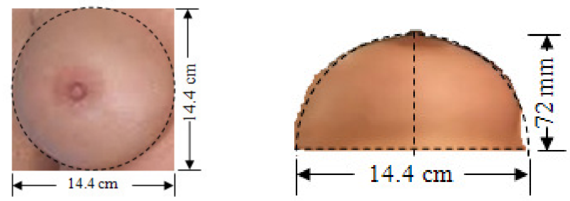

Fig. 1: Breast Geometry

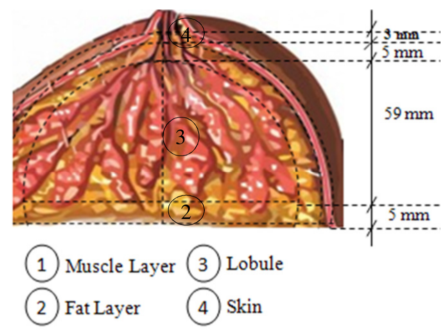

Fig. 2: Breast Cross-section

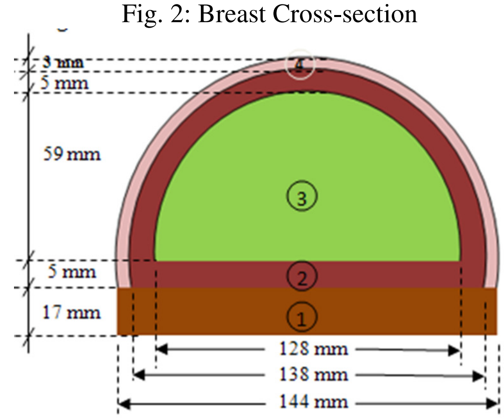

Fig. 3: Breast Model (2D)

Analysis of thermal features on breast requires a realistic (anatomical accurate) physical (geometric) model which should be developed mimicking the structure and the heterogeneity. The outlook of a natural breast is shown in Fig. 1 (source:www.cancer.gov). Studies assume that average adult breast is grown on a circular base of radius 144 mm and height 72 mm referring a natural, un-deformed breast, basically, to hemispherical view [10]. Further, developing a realistic model requires identifying the subdomains, which necessitates inspecting the breast anatomy. Anatomic studies discovered that female breast build with eight different tissue layers including the skin surface [10]. The cross-sectional diagram of a breast shown in Fig. 2 (source:www.commons.wikimedia.org), however, indicates the major domains because the sizes of the disregarded tissue layers are minute and pointless to pay heed to investigate the thermal character. The domains are roughly demarked with dotted lines and their respective thicknesses are labeled at right. The hemisphere shaped lobule tissues layer is sandwiched in fat layer. The upper fat layer is covered by skin layer and the bottom fat layer is grown on muscle layer (not shown in the figure). For a breast of 7.2 cm radius, the thickness of thoracic wall and muscle are 7 and 10 mm respectively, the radius of lobule is 59 mm and the thickness of fat layer is 5 mm, discovered in [10].

Development of realistic breast model (2D) in Fig. 3, the minute tissues such as the nipple, areola and milk ducts are not considered. The model considers the chest wall tissues (muscles) as a solid rectangle and the lobule and fat layers as hemispheres with an inserted fat layer between the muscle and lobule layers. The 3D breast model is developed by revolving the Fig. 3 around the vertical axis which is shown in Fig. 4. In the figure the bottom circular disc (pink color) of radius 7.2 cm and thickness of 17mm is determined for muscle tissues and two hemispheres of radii 6.4 and 6.9 cm indicate outer boundaries for the lobule (green color) and fat layer (blue color), respectively [13, 14]. In addition a spherical hot nodule (red color) is inserted into the lobule layer. The physical (size and position) as well as the bio-thermal parameters of the nodule have to change to provide training vector sets for the study.

Thermal study of breast tumor also requires understanding the heat-exchange features at the boundaries which are following:
The bottom boundary (the chest wall):

$$T(r) = T_b \tag{2}$$

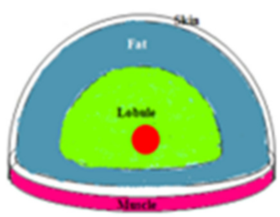

Fig. 4: Breast Model (3D)

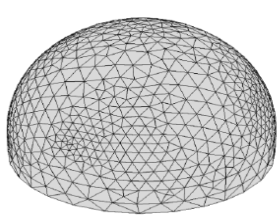

Fig. 5: Finite Element Model

The inter-domain boundaries (fat-muscle, fat-lobule, lobule-tumor etc.) are thermally insulated:

$$-\lambda_{i,j}\frac{dT}{dn} = 0 \tag{3}$$

And the perimeter of the outer hemisphere (covered by skin) undergoes to the following convection and radiation heat loss:

$$-\lambda_4\frac{dT(r)}{dn} = \alpha(T(r) - T_a) \tag{4}$$

where α is the heat transfer coefficient and T_a is the ambient temperature.

3. Numeric Model

Above stated thermal problem is to be solved with help of FEM which requires producing a finite element model of the breast as presented in Fig. 5. The entire breast model with tumor is divided into approximately 96000 tetrahedral, and around the boundaries 24000 triangular elements. In addition, nodes along the surface area constrained in the normal-translational direction. All other nodes are unconstrained in all directions. A constant temperature of 20° C has applied at the entire section as an initial condition. The maximum and minimum element sizes are chosen as 1 cm and 0.2 mm, respectively. The maximum element aspect ratio is 1.5. Assuming the subdomain 1, 2, 3, 4 and 5 for the muscle, fat layer, lobule, skin and hot nodule, respectively, the boundary conditions are to be linked as well as their thermal and physiological parameter are to be defined. The thermal and physiological parameters for different subdomains are listed in Table 1 [7-10, 15].

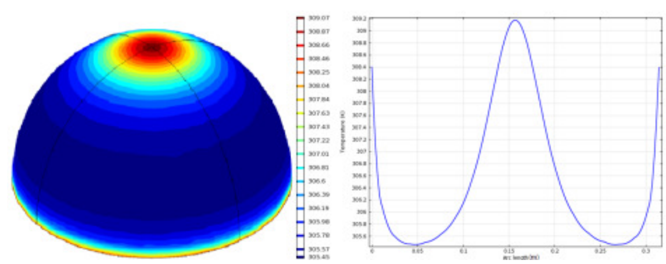

Fig. 6: Surface Temperature pattern; on overall breast (left), and directly above the tumor center (right)

The numerical model has been solved for all possible tumor types, for example, deep seated to shallow body tumors and benign to malignant tumors to produce a set of idealized training vectors for training the ANN. To exemplify, the temperature profile for a midway (depth 30 mm), midrange (radius 12 mm and metabolic rate 40kW/m^3) tumor is presented in Fig. 6. The figure shows that 3° elevation of temperature occurs at a point which is directly above the center of the tumor and temperature grows over a circular region of radius 10 mm.

4. Inverse Problem and Result

Numeric analyses reveal that the physical and thermal parameters of tumors cause a hot zone at the regional skin surface directly above the tumor. Now, the idea is utilizing the anomalous skin surface temperature for predicting the location, size and heat generation rate of the tumor; this has been performed using the evolutionary method involving the ANN and the PSM as shown in Fig. 7. The ANN is used to map the relationship of tumor depth, size and heat generation rate to the temperature profile over the realistic breast model. Temperature profiles obtained from ANN is then validated with numerical data before applying it to estimate tumor parameters [7, 10].

Table 1: Thermal and physiological parameters

Domain	Parameter	Value and Unit
Muscle (1)	k	0.48 W/m.K
	ω_b	5.7×10^{-4} 1/s
	Q_m	700 W/m^3
Fat layer (2,4)	k	0.21 W/m.K
	ω_b	3.8×10^{-4} 1/s
	Q_m	400 W/m^3
Lobule (3)	k	0.48 W/m.K
	ω_b	5.7×10^{-4} 1/s
	Q_m	700 W/m^3
Tumor (5)	k	0.65 W/m.K
	ω_b	11.5×10^{-3} 1/s
	Q_m	14000 W/m^3
Whole (1,2,3,4 and 5)	c_b	4186 J/m^3. K
	ρ_b	1000 kg/m^3
	T_a	36.15°C
	T_e	26.6 °C
	h_a	8.77 W/m^2

A multilayer feed-forward ANN with back propagation learning algorithm is established in MATLAB with the Neural Network Toolbox using the 'newff' function. After some experimentation, the transfer function 'trainlm' has chosen for both the hidden layers and the output neurones. The network has three input nodes for three parameters that are being investigated, and 46 output nodes that express one half of the symmetrical temperature profile on the skin exterior. There are two hidden layers for the network, the first layer has 33 nodes and the second layer has 25 nodes. Therefore, a 3-33-25-46 neural network architecture was developed, trained and tested to validate the model.

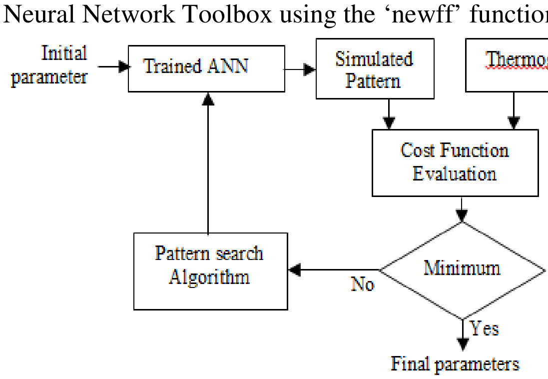

Fig. 7: Estimation process

Then, the PSM has been applied for computing the thermal and physical parameters of tumor by minimizing fitness (cost) function [7, 16-18]. The fitness function relates the given data to the temperature profile for a given set of estimated parameters. The objective function is defined as:

$$E = \sum |T_{IR} - T_{sim}(d, R, Q_m)| \quad (5)$$

where T_{IR} and T_{sim} are the vectors that contains thermogram (numerical simulation data) and estimated temperature data, respectively.

Confining the solutions to a meaningful range, assuming the solution domain, $\Gamma \subset \{d, Q_m, R\}$ parameters follow some constraints, for example the depth depends on the body geometry and may have diverse ranges between 0.5 and 5 cm; the heat rate between ten and hundred kilowatt per unit volume; and the radius between 9 and 35 mm (T1 and T2 stage tumor). A simple and efficient way to fit the assorted elements for the PSM is to define a dimensionless vector as:

$$\Gamma_n = \begin{cases} d_n \\ Q_{mn} \\ R_n \end{cases}$$

where $\Gamma_n \in \mathbb{R}, 1 \le \mathbb{R} \le 2$, is the dimensionless domain and d_n, Q_{mn} and R_n are the dimensionless depth, heat rate and radius, respectively.

The search method requires defining a column matrix of initial value and positive step-size parameter as:

Let $\chi^0 = \begin{vmatrix} d_n \\ Q_{mn} \\ R_n \end{vmatrix} \varepsilon\, \Gamma_n$ and $\Delta_0 > 0$ and a direction matrix

$$P_k = \begin{vmatrix} 1 & 0 & 0 & 1 & 1 & 0 & 1 & -1 & 1 & 1 & -1 & 1 & -1 & -1 & 0 \\ 0 & 1 & 0 & 1 & 0 & 1 & 1 & 1 & -1 & 1 & -1 & -1 & 1 & -1 & 0 \\ 0 & 0 & 1 & 0 & 1 & 1 & 1 & 1 & 1 & -1 & 1 & -1 & -1 & -1 & 0 \end{vmatrix}$$

Then the process goes in the following way:

For $k = 0, 1, 2, \dots ....$

For $i = 0, 1, 2, \dots \dots 7,$

a) Compute$\left\| T_a - T_s^k(d, Q_m, R) \right\|$.

b) Determine s_k abiding by $s_k \epsilon \Delta_k P_k$, $(x_k + s_k) \in \Omega$ and$\left\| T_a - T_s^k(d, Q_m, R) \right\| >$ $\left\| T_a - T_s^{k+1}(d, Q_m, R) \right\|$ and perform step (a). For all values of i compute min $\left\| T_a - T_s^k(d, Q_m, R) \right\|$ and find X^{k+1} and $\Delta_{k+1} = \Delta_k/2$ (keep not less than 0.005). Otherwise X remain unchanged and $\Delta_{k+1} = 2\Delta_k$.

Selection of X^0 and Δ_0 can lead to local or global minima after reasonable iterations. Several random choices of $X^0$and their respective $\Delta_0$was recommended to ensure the global minima.

Finally, the actual domain parameters can be reproduced from the dimensionless parameters using:

$$\mathcal{X} = (\mathcal{X}_{max} - \mathcal{X}_{min})(\mathcal{X}_n - 1) + \mathcal{X}_{\min} \quad (6)$$

where $\{\mathcal{X}, \mathcal{X}_{max}, \mathcal{X}_{min}\} \epsilon \Gamma$, $\Gamma \subset \{d, Q_m, R\}$ and $\{\mathcal{X}_n\} \epsilon \Gamma_n$.

The results obtained using these methodologies for solving the inverse problem related with tumors located in breast are listed in Table 2 & Table 3. The parameters estimated from ideal surface temperature data of different tissue types are presented in Table 2. For each cases the developed methodology is run with different random initial sets, but the final estimates are identical regardless the initial population. These results show a good agreement between the actual and forecasted parameters, with maximum absolute error in heat generation rate of only 3% for the tumor embedded in lobule region in breast. Moreover, when a random noise $\leq \pm 10\%$ is added to the input data the results obtained are in good agreement between the actual and forecasted parameters as presented in Table 3. In all cases the values of the known parameters and dimensions of the domain are same as presented in section 3.

It can be seen that using the proposed methodology it is possible to determine the depth, radius and heat generation of tumor with a good accuracy.

Table 2: Estimation of thermal and physical parameters of tumor (Noiseless System)

Actual Data			Run	Noiseless			Maximum Error
Depth (cm)	Heat Rate (W/m^3)	Radius (mm)		Depth (cm)	Heat Rate (W/m^3)	Radius (mm)	
2.5	40000	9	1	2.5123	41197	8.7934	3%
			2	2.5023	41346	8.9103	
			3	2.4997	39456	9.1405	

Table 3: Estimation of thermal and physical parameters of tumor (Noisy System)

Actual Data			Run	±5-10 % Noise			Maximum Error
Depth (cm)	Heat Rate (W/m^3)	Radius (mm)		Depth (cm)	Heat Rate (W/m^3)	Radius (mm)	
2.5	40000	9	1	2.5426	40197	8.7845	6.1%
			2	2.5236	38346	8.804	
			3	2.4788	42450	9.125	

5. Conclusion

A methodology has developed for the estimation of thermophysical or geometrical parameters of tumor region using the temperature profile on the skin surface that may be acquired by infrared thermography. The problem is solved using finite element method on realistic model of breast with considering its thermal inhomogeneity to produce realistic thermal dataset over the surface. A neural network is trained with the dataset for establishing a correlation between the surface temperature profile and the thermo-physical parameters of tumor. In the inverse problem, the temperature graph is fitted using the trained ANN for a predicted solution vector where the vector includes the variables, such as the depth, size and metabolic rate of a tumor. In a given search domain the predicted parameters are found by searching around with the PSM and finally converged to the optimized values where the cost function is minimum. The optimum solution is picked up for the locating a tumor which grow in lobule tissues. The estimated results are consistent and evidently demonstrate the feasibility of the proposed methodology. Even in case of noisy system ($\leq \pm 10\%$) the methodology estimates the bio-thermal and physical parameters with a very good accuracy. The same parameters were estimated with 3% and 8% error for noiseless and noisy system, respectively in [7] for homogeneous cuboid tissue model. With comparing to that the results obtained in this study is more accurate and relevance as it is estimated on anatomic accurate breast model.

Therefore, it is evident that the developed methodology can accurately determine the tumor's depth, size and hyperactivity rate which is embedded in the lobule tissues of breast. The predicted features could be useful for clinic diagnosis, hypothermia ablution as well as for studying tumor evolution during a treatment procedure. However, the proposed methodology has not validated with real dataset, consequently can be applied on patients only to determine the progress of treatments by computing the thermal features of tumours as an adjunctive tool with the existing techniques.

References

[1] http://www.cancer.org/cancer/breastcancer/overviewguide/breast-cancer-overview-survival-rates

[2] J. Chato, Measuement of thermal properties of biological materials, in: A Shitzer, RC. Eberhart (Eds.), in: Heat transfer in Medicine and biology, vol. 1, Plenum Press, NY, 1985, pp. 167-173.

[3] H. F. Bowman, Estimation of tissue blood flow, in: A Shitzer, RC. Eberhart (Eds.), in: Heat transfer in Medicine and biology, vol. 1, Plenum Press, NY, 1985, pp. 193-230.

[4] M. M. Chen, C.O. Pedersen, J. C. Chatro, On the feasibility of obtaining three dimensional

information from thermographic measurements, ASME Journal of Biochemical Engineering 99 (1977) 58-64.
[5] R. N. Lawson, M. S. Chugtai, Breast Cancer and body temperatures, Canadian Medical Association Journal 88 (1963) 68-70.
[6] R. N. Lawson, Implication of surface temperatures in the diagnosis of breast cancer, Canadian Medical Association Journal 75 (1956) 309-310.
[7] J. P. Agnelli et al., Tumor location and parameter estimation by thermography, Mathematical and Computer modeling (2010), doi: 10.1016/j.mcm. 2010.04.003.
[8] Manu Mital and E. P. Scott, Thermal detection of embedded tumours using infrared imaging, in ASME J. of biomechanical eng., vol. 129, 2007, pp. 33-39.
[9] Manu Mital and Ramana M. Pidaparti, Breast tumour simulation and parameters estimation using evolutionary algorithm, in Hindawi publishing center, modeling and simulation in engineering, vol. 2008, doi: 10. 1155/2008/756436.
[10] Sudarshan, N. M., Ng, E. Y. K., and Teh, S. I., Surface Temperature Distribution of a Breast with and without Tumor, Comput. Methods Bio-mech. Biomed. Eng., 2, pp. 187–199, 1995.
[11] S. Hossain, F.A. Mohammadi and E.T. Nezad, Neural network approach for the determination of heat Source parameters from the surface temperature image, in Proceedings of the 24th Canadian Conference on Electrical and Computer Engineering: 8-11May 2011; pp. 1109-1112.
[12] H.H. Pennes, Analysis of tissue and arterial blood temperatures in the resting human forearm. *J. Appl. Physiol.* **1** (1948), pp. 93–122.
[13] Ng EYK, Sudharan NM, An improved tree-dimensional direct numerical modeling and thermal analysis of a female breast with tumor. Proc Inst Mech Eng Part H- J Eng Med 2001; 215:25-37.
[14] Ng EYK, Sudharan NM, Numerical uncertainty and perfusion induced instability in bioheat equation: its importance in thermographic interpretation J Med Eng Tech 2001; 25:222-9.
[15] E. F. J. Ring, Progress in the measurement of human body temp., IEEE Eng. Med. Biol. 17(4) (1998) 19-24.
[16] R.M. Lewis, V. Torczon, Pattern search algorithms for bound constrained minimization, SIAM Journal on Optimization 9 (4) (1999) 1082–1099.
[17] V. Torczon, On the convergence of Pattern Search Algorithms, SIAM J. on Optimization 7(1)(1997) 1-25.
[18] R.M. Lewis, V. Torczon, Pattern search methods for linearly constrained minimization, SIAM Journal on Optimization 10 (3) (2000) 917–941.